Optics Letters

Holographically fabricated out-of-plane blazed gratings and channel waveguides in silica for integrated free-space beam delivery

Q. Salman Ahmed, Paul C. Gow,* James W. Field, Dong-Woo Ko, Rex H. S. Bannerman, Peter Horak, Christopher Holmes, Peter G. R. Smith, Corin B. E. Gawith, and James C. Gates

Optoelectronics Research Centre, University of Southampton, Southampton SO17 1BJ, UK
**p.gow@southampton.ac.uk*

Received 30 July 2024; revised 27 September 2024; accepted 18 October 2024; posted 21 October 2024; published 8 November 2024

Grating couplers are widely used in integrated optics to generate free-space beams and facilitate localized interactions with systems such as atom or ion traps. However, etched devices often exhibit small-scale inconsistencies; exacerbated by the high index contrast of the devices, this can lead to phase errors, limiting devices to a sub-millimeter scale. Here we present the first demonstration, to our knowledge, of tilted, out-of-plane blazed gratings in planar silica fabricated by UV inscription using a 213 nm laser. Our devices deliver collimated and focusing beams into free space from a waveguide input without the need for additional optics such as beam expanders.

https://doi.org/10.1364/OL.537811

Chip-scale photonic devices have significantly progressed fundamental investigations in atomic physics [1], time/frequency metrology [2], and biology [3] while also finding utility in industrial sectors such as telecommunications [4,5] and light detection and ranging (LIDAR) [6]. In many applications, the effective integration of nanophotonic circuits with purposefully designed, free-space optical fields in millimeter-scale volumes has substantially expanded the potential for chip-scale, highly integrated sensors and systems. For instance, the National Institute of Standards and Technology (NIST) is presently engaged in the deployment of chip-scale photonic systems featuring integrated atomic vapor cavities [1]. Realizing the complete potential of these systems necessitates advancements in compact, precise, and efficient optical connections from few-micrometer-wide photonic waveguides to mm-scale free-space beams.

Silicon nitride (SiN) and silicon-based etched grating couplers are the most commonly recognized materials for interfacing a guided mode with a radiation mode for various applications in atom/ion traps, biological sample detection, and sensing. For instance, Mehta *et al.* [7] demonstrated an ion trap design based on lithographically defined nanophotonic waveguides for guiding light and addressing Sr^+ ions in an integrated chip. The waveguides were fabricated on a quartz substrate in a SiN film for a single-mode operation at $\lambda = 674$ nm with a TE polarization. The same group has also presented a compact design and characterization of grating couplers to focus beams out of plane [8]. Becker *et al.* [9] demonstrated an integrated waveguide with gratings that couple a 1550 nm light from a single-mode waveguide-to-free-space and also a one-dimensional focusing grating coupler to project a linearly polarized light out of the plane. Kim *et al.* [10] demonstrated an integrated SiN grating with free-space beam coupling out of the plane. Their design consisted of a mode converter providing an interface between the photonic mode in the waveguide and the free-space beam. The same research group presented a modified scheme [11] where Si metasurfaces were added to the top of the etched grating footprint to focus to a 475 nm spot (FWHM). Kerman *et al.* [3] investigated an integrated SiN photonic circuit that could excite and collect fluorescence from microparticles flowing in a microfluidic channel. The structure comprised one focusing grating coupler (FGC) for fluorescence excitation and three other FGCs for collection. For ease of comparison, these results are summarized in Table 1 along with the parameters from this work.

Etched gratings are promising in terms of coupling efficiency from a guided mode to free space. However, the lithographic and etching processes often require stringent phase-matching conditions. This, coupled with the high refractive index contrast of etched gratings, can limit the size of grating components to the sub-mm scale. As demonstrated in Table 1, these devices typically have small beam widths with close working distances to the focus (tens of microns) and are targeted toward interactions with individual atoms, ions, or particles. For larger beams, it is then necessary to expand these beams using optics or metasurfaces. It is desirable to fabricate grating couplers capable of generating 10 mm or larger-sized free-space beams, as well as focusing beams, for direct coupling into atom trap systems. Recognizing the limitations of lithography and etching, researchers have explored alternative methods of fabricating waveguide-to-free-space couplers in planar silica, such as the phase mask techniques [12] and direct writing approaches, including femtosecond [13] and

Table 1. Summary of Prior Art

Platform	Grating Dimensions	Focal Distance
SiN [7]	18 × 18 μm (2D)	50 μm
SiN [8]	18 × 18 μm (2D)	50 μm
SiN [10]	300 × 250 nm (2D)	Collimated
Si-on-insulator [9]	10 × 10 μm (2D)	4 μm
SiN [11]	200 μm (1D)	75 μm
SiN [3]	6.2 μm (1D)	11 μm
SiO_2 [this work]	2 mm (1D)	4.8 mm

UV laser writing [14]. Silica as a platform is desirable, as the low index contrast of the gratings allows for larger grating areas, and its transparency in the visible and near-infrared permits many different wavelengths as well as the potential for imaging through the coupling device. Femtosecond writing provides a unique ability to inscribe 3D photonic structures independent of the photosensitivity of a silica glass [13]. However, the refractive index change is based on nonlinear avalanche ionization which can result in non-uniform grating profiles. The use of phase masks is a common technique to define different types of gratings into an optical fiber core upon UV exposure [12], but relies upon a pre-existing waveguide. In contrast, small spot UV writing represents a more flexible approach to defining waveguides and gratings in a planar silica. Recent results have shown that a 213 nm pulsed laser source can be used for waveguide and Bragg grating inscription with and without hydrogen loading, further simplifying this approach [15–19].

In this Letter, we demonstrate the first silica-based out-of-plane grating coupler fabricated by phase controlled dual-beam interferometry. Our SiO_2 on Si substrates were fabricated using the flame hydrolysis deposition (FHD) to deposit a core layer of a boron-/germanium-doped silica with a thickness of 3.3 μm onto the 15 μm thick thermal oxide on top of a silicon substrate. This core layer was subsequently capped via the FHD with a cladding layer of a boron-/phosphorous-doped silica, measuring 17.7 μm in thickness. The wafer was then diced into chips measuring 20 × 10 mm, which were subsequently loaded into a hydrogen cell at 120 bar pressure for 5 days to enhance the photosensitivity of the core layer. Waveguide and grating fabrication was performed using a small spot interferometer, which simultaneously inscribes the waveguide and gratings at a 45° blaze angle with respect to the normal.

The 45° blaze angle provides the directionality required to outcouple the guided mode to free space. However, the fabrication of gratings in a planar silica with a blaze angle of 45° relative to the normal of the chip surface presents a challenge when employing dual-beam interferometry. The challenge comes from the large angles of the incident UV beams, resulting in significant Fresnel losses and making it impossible to couple the incident UV beams into silica at the necessary angles to produce gratings with the desired 45° blaze angle. In order to overcome this limitation, we introduced a prism coupling mechanism [20,21] to reduce the Fresnel losses and power imbalance in the two beams as shown in Figs. 1 and 2 .

Figure 1 illustrates the alignment of the two beams and how they are brought together to interfere, generating a fringe pattern at an angle of 45° with respect to the normal surface of the chip. One arm of the interferometer is at an angle of 28.7° to the chip normal and is considered beam A, while the other arm is at a larger angle of 61.3° to the chip normal and is called beam B. Loss of power in terms of reflection from one medium to another can be calculated using the Fresnel coefficients. When introducing a prism, the Fresnel losses are minimized due to the smaller angle of incidence to the prism surface normal compared to the chip surface normal. After passing through the prism, both beams are focused into the B-/Ge-doped core layer of the FHD substrate. Between the surface of the prism that remains static and the FHD silica chip that translates beneath, an index-matching fluid (de-ionized water) is introduced. By utilizing the above methodology, both beams exhibit ~9% of power loss for the *s*-polarized light, delivering optimal UV power to the photosensitive core and offering the potential for high contrast refractive index gratings.

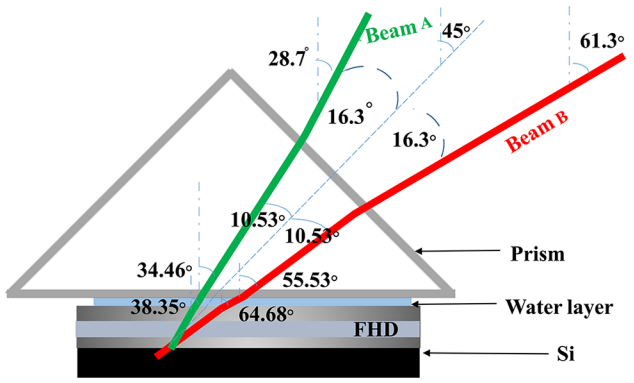

Fig. 1. Diagram of the Fresnel reflections at the surface of the prism, water, and FHD silica when the beams of a 213 nm laser interferometer are incident.

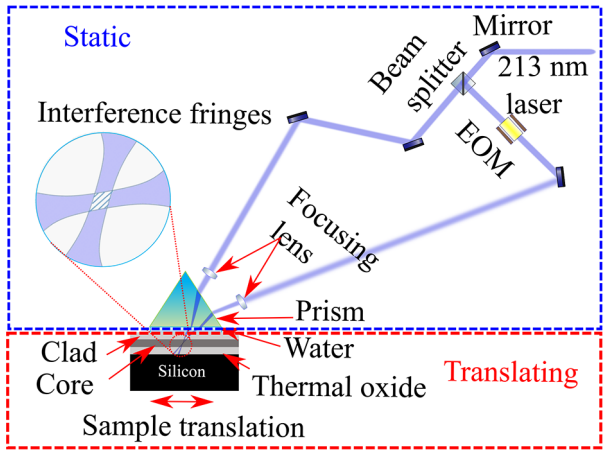

Fig. 2. Schematic of the direct 213 nm writing system to inscribe out-of-plane 45° blazed gratings using a 213 nm laser.

Using the beam arrangement in Fig. 1, a laser interferometer was designed to generate 45° blazed gratings by dual-beam UV writing as shown in Fig. 2. Our 213 nm laser writing beam is split into two arms by a 50:50 beam splitter. One arm of the interferometer is passed through a DKDP electro-optic modulator (EOM) (Leysop Ltd.) to provide phase control of the interference pattern. A pair of CaF_2 lenses were used to focus the beams to a $1/e^2$ diameter of 7.6 μm. A right-angled UV silica prism was mounted on a rail, and a ~100 μm layer of de-ionized water was introduced to approximate index matching between the substrate and the prism. A bespoke vacuum chuck was used to hold the chip and store sufficient water for several

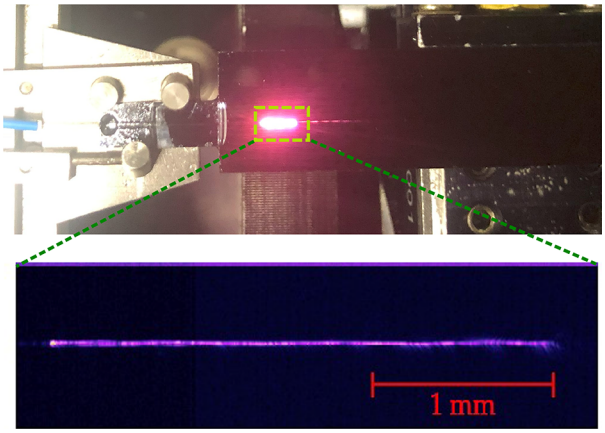

Fig. 3. (a) Photograph of the fabricated chip coupled with a fiber V-groove assembly. This photograph was taken from a CMOS phone camera. (b) Close-up image of the 780 nm light coupling out of a single 3 mm long uniform grating. The image was taken using a Spiricon beam profiler.

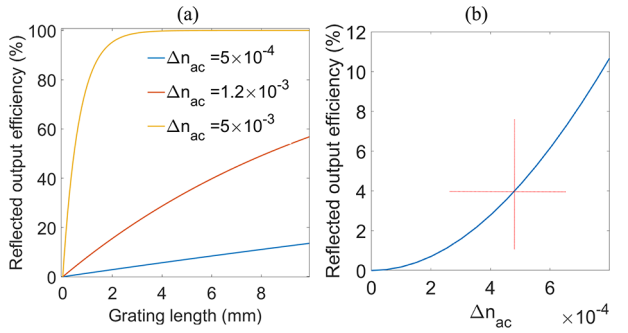

Fig. 4. (a) Analytically calculated output efficiency from a 45° blazed grating against the grating length at Δn_{ac} of 0.5×10^{-3}, 1.2×10^{-3}, and 5×10^{-3}. (b) Reflected output efficiency versus Δn_{ac} for a 3 mm long uniform grating. A 4% or −13.9 dB efficiency was experimentally achieved.

hours of fabrication. During the fabrication, the prism was static, and the sample was translated using precision air-bearing stages (Aerotech ABL9000).

Channel waveguides were fabricated containing 45° blazed gratings (1D out-of-plane grating coupler) at a period of ∼530 nm to couple a 780 nm light out of the chip, normal to the surface. First, a 3 mm long grating with a uniform apodized profile was inscribed by modulating the phase of the beams via the EOM. We characterized the device by launching a 780 nm light into the channel waveguide using a fiber V-groove assembly, a photograph of which is shown in Fig. 3(a). Through the 45° blazed grating, the guided mode was coupled into free space and was analyzed by a Spiricon BeamGage camera, as shown in Fig. 3(b). The coupled output efficiency (fiber-to-free space) was measured to be −14 Spiricon BeamGage dB for a 3 mm long uniform grating.

We performed analytical modeling [22] to calculate the expected output efficiency from a 45° blazed grating versus the grating length with modulated refractive indices (Δn_{ac}) of 0.5×10^{-3}, 1.2×10^{-3}, and 5×10^{-3}, and the results are shown in Fig. 4(a). According to these calculations −14 dB or 4% reflected output efficiency corresponds to Δn_{ac}=0.48×10^{-3} for our gratings, as shown in Fig. 4(b).

Further to this experiment, a second chip was written with a chirped grating profile designed to bring the outcoupled free-space beam to a focus. The grating was 2 mm long, with a Gaussian apodized profile, and was designed to focus 5 mm above the surface of the chip. The local period was numerically calculated to ensure all rays diffracted along the waveguide meet at a common focus, compensating for the glass/air refraction. This is a subtle nonlinear function and is necessary due to the gratings' buried nature and the focused beam's high numerical aperture [23].

Characterization of the beam coupling profile from our 2 mm long chirped grating was performed by taking several images at steps of 100 μm in the z axis above the plane of the device using the Spiricon BeamGage. Figure 5(a) shows a schematic diagram of the beam focusing above the surface of the blazed chirped grating. Figure 5(b) shows the characterized beam focusing (in the x direction), where the image slices were summed and normalized in the non-focusing direction. The planar waveguide substrate was not optimized for a 780 nm single-mode operation and demonstrated an additional vertical higher-order mode. This introduces beating and the angular fringes observed in Fig. 5(b). The beam waist is indicated by a dashed orange line, and a linear plot at a beam waist of ≈23 μm close to the focus is shown in Fig. 5(c) to illustrate the quality of the beam. The focused beam waist was measured as 4.6 ± 0.2 μm with a focal length of 4.8 ± 0.1 mm. Based on theoretical calculations, the focused spot diameter of a 2 mm wide Gaussian beam should be ≈2.4 μm. However, the experimentally measured beam waist is twice the calculated value; this is again likely due to the multimode nature of the waveguide. The reflected output efficiency (fiber-to-free space) was −20 dB with a calculated Δn_{ac} of 0.24 $\times 10^{-3}$. Figure 5(d) shows the beam propagation from the same grating in the y (non-focusing) direction, where the image slices were summed in the focusing direction. The beam diffracted as expected from a 7 μm wide channel waveguide. Figure 5(e) shows a linear plot of the region close to the grating, indicated by the dashed orange line in (d). This essentially shows the quality of the mode as it emerges from the grating.

Although the reflected output power of our fabricated devices was between −20 and −14 dB, it is expected that we can significantly improve the efficiency of these devices. Firstly, ensuring the fabricated core layer permits only a single-mode propagation for 780 nm, and that this matched to the launch optical fiber for efficient coupling. The second key factor is improving the refractive index contrast of the grating (Δn_{ac}), which has a strong quadratic dependence on reflectivity. To date, investigations suggest that the grating quality can be improved by optimizing the interferometric system—primarily beam intensity balancing and co-alignment, as well as air current stabilization. By accessing the current maximum experimentally achieved Δn_{ac} for our system (1.25×10^{-3}) [16], the resulting coupling efficiency would be 60% for a 10 mm long blazed grating. Assuming the same Δn_{ac}, future 2D out-of-plane gratings would demonstrate the same efficiency as the first 1D geometry. Fabrication potentially becomes simpler due to the larger spot sizes afforded by the larger writing area, with an associated improved grating quality (Δn_{ac}). It is worth noting that writing times would not drastically increase as the writing power could be increased in line with the reduced power density, whereas in this Letter, we are restricted by the small spot size required to produce a single-mode waveguide. However, a 2D system would require an

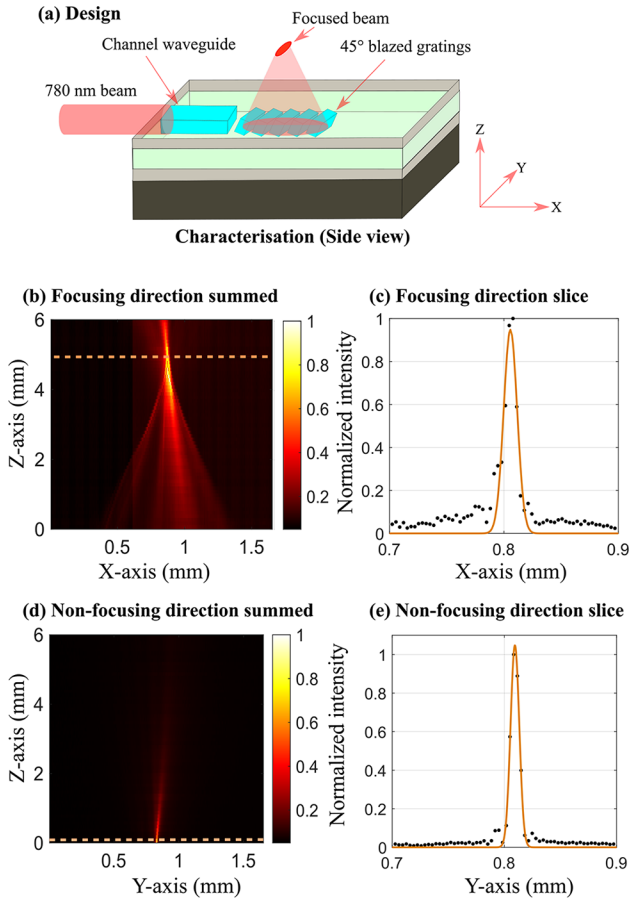

Fig. 5. (a) Schematic of a 1D grating coupler showing an out-of-plane beam focusing from a chirped blazed grating. (b) Characterized summed image of the light focusing out of the chip in the x (focusing) direction from a 2 mm chirped blazed grating. (c) Linear plot of an image slice near the focus showing the beam quality (dashed orange line in (b)). (d) Characterized summed image of the light diffracting from the same grating in the y (diverging) direction. (e) Linear plot of an image slice close to the grating (dashed orange line in (d)).

in-plane dispersive element, such as a grating [23] or evanescent coupler [10], and this will reduce the total device efficiency.

In this Letter, we have introduced a compact fiber-coupled integrated approach for delivering large collimated and focused free-space beams for quantum technologies. We have demonstrated the first out-of-plane silica-based grating coupler fabricated using a state-of-the-art holographic writing system. Using a prism coupling approach, we developed a new interferometer to inscribe out-of-plane 45° blazed gratings in a silica-on-silicon platform. A characterization system was established to analyze the light coupling out of plane into free space. A maximum reflected output efficiency of −14 dB was achieved for a 3 mm long uniform grating. We also demonstrated a focusing grating coupler by introducing a chirp profile to the 45° blazed gratings. Chirped gratings were characterized by taking several scans by a Spiricon BeamGage using a computer-controlled translation stage. Results showed the beam focusing to a waist of 4.6 ± 0.2 μm at a distance of 4.8 ± 0.1 mm above the surface. In the future, we will expand this fabrication approach toward longer gratings, with increased Δn_{ac} to improve the efficiency of optical outcoupling. Real-world devices will require 2D gratings to create large area collimated and focusing beams. Therefore, the ongoing work will explore utilizing a slab waveguide for in-plane expansion and 2D out-of-plane gratings for coupling to free space.

Funding. Royal Academy of Engineering (Research Chair - Corin Gawith); Innovate UK (50414); Engineering and Physical Sciences Research Council (EP/M013294/1, EP/M013243/1, EP/M024539/1, EP/T001062/1, EP/V053213/1, EP/T00097X/1).

Disclosures. The authors declare no conflicts of interest.

Data availability. Data underlying the results presented in this paper are available in Ref. [24].

REFERENCES

1. M. T. Hummon, S. Kang, D. G. Bopp, *et al.*, Optica **5**, 443 (2018).
2. T. J. Kippenberg, R. Holzwarth, and S. A. Diddams, Science **332**, 555 (2011).
3. S. Kerman, D. Vercruysse, T. Claes, *et al.*, ACS Photonics **4**, 1937 (2017).
4. D. Thomson, A. Zilkie, J. E. Bowers, *et al.*, J. Opt. **18**, 073003 (2016).
5. J. Chovan and F. Uherek, Radioengineering **27**, 357 (2018).
6. J. Sun, E. Timurdogan, A. Yaacobi, *et al.*, Nature **493**, 195 (2013).
7. K. K. Mehta, C. D. Bruzewicz, R. McConnell, *et al.*, Nat. Nanotechnol. **11**, 1066 (2016).
8. K. K. Mehta and R. J. Ram, Sci. Rep. **7**, 2019 (2017).
9. H. Becker, C. J. Krückel, D. V Thourhout, *et al.*, IEEE J. Sel. Top. Quantum Electron. **26**, 8300408 (2020).
10. S. Kim, D. A. Westly, B. J. Roxworthy, *et al.*, Light: Sci. Appl. **7**, 72 (2018).
11. A. Yulaev, W. Zhu, C. Zhang, *et al.*, ACS Photonics **6**, 2902 (2019).
12. M. Gagné and R. Kashyap, Opt. Commun. **283**, 5028 (2010).
13. M. Lancry, B. Poumellec, J. Canning, *et al.*, Laser Photonics Rev. **7**, 953 (2013).
14. Q. S. Ahmed, P. C. Gow, P. L. Mennea, *et al.*, *Integrated Photonics Research, Silicon and Nanophotonics* (Optical Society of America, 2020), paper IW2A.4.
15. P. C. Gow, R. H. S. Bannerman, P. L. Mennea, *et al.*, Opt. Express **27**, 29133 (2019).
16. Q. S. Ahmed, J. W. Field, C. Holmes, *et al.*, Opt. Mater. Express **13**, 495 (2023).
17. Q. S. Ahmed, P. C. Gow, C. Holmes, *et al.*, Electron. Lett. **57**, 331 (2021).
18. P. C. Gow, Q. S. Ahmed, P. L. Mennea, *et al.*, Opt. Express **28**, 32165 (2020).
19. P. C. Gow, Q. S. Ahmed, J. C. Gates, *et al.*, Opt. Mater. Express **11**, 1835 (2021).
20. S. M. Schultz, T. K. Gaylord, E. N. Glytsis, *et al.*, "Diffractive grating coupler and method," U.S. patent 6,285,813 (9 September 2001).
21. S. M. Schultz, E. N. Glytsis, and T. K. Gaylord, Appl. Opt. **39**, 1223 (2000).
22. D.-W. Ko, Q. S. Ahmed, J. W. Field, *et al.*, Opt. Express **30**, 44628 (2022).
23. J. W. Field, S. A. Berry, R. H. Bannerman, *et al.*, Opt. Express **28**, 21247 (2020).
24. A. Salman, J. Feild, D.-W. Ko, *et al.*, "Dataset in support of the article 'Holographically fabricated out-of-plane blazed gratings and channel waveguides in silica for integrated free space beam delivery'," University of Southampton Institutional Repository (2024), https://doi.org/10.5258/SOTON/D2913.